

Electronic structure of the spin- $\frac{1}{2}$ chain compound MgVO_3

I. Chaplygin and R. Hayn

Institute for Theoretical Physics, TU Dresden, D-01062 Dresden, Germany

K. Koepnik

Max Planck Institute CPFS, D-01187 Dresden, Germany

(Received 25 June 1999)

Band-structure calculations with different spin arrangement for the spin-chain compound MgVO_3 have been performed, and paramagnetic as well as magnetic solutions with ferro- and antiferromagnetically ordered chains are found, the magnetic solutions being by 0.22 eV per formula unit lower than the paramagnetic one. The orbital analysis of the narrow band crossing the Fermi level in the paramagnetic solution reveals that the band has almost pure vanadium 3d character, the lobes of the relevant *d* orbitals at the neighboring in-chain sites being directed towards each other, which suggests direct exchange. The tight-binding analysis of the band confirms the strong exchange transfer between neighboring in-chain V ions. Besides, some additional superexchange transfer terms are found, which give rise both to in-plane coupling between the chains and to frustration, the dominant frustration occurring due to the interchain interactions. [S0163-1829(99)51242-3]

Spin chains and ladders are of fundamental interest for solid-state physics due to their peculiar properties.¹ In the last years many spin-chain compounds were found, mostly cuprates¹⁻³ and vanadates.⁴ There one can distinguish between the corner-sharing compounds with a 180° transition metal(T)–ligand(L)–T bond [Sr_2CuO_3 (Refs. 2 and 5)] and the edge-sharing compounds with a 90° T-L-T bond [Li_2CuO_2 , CuGeO_3 (Ref. 3), and MgVO_3 (Ref. 4)]. In cuprates the relevant *d* orbitals are directed towards the ligand ions, which results in a strong antiferromagnetic superexchange interaction for a 180° T-L-T bond and a weaker ferromagnetic coupling for a 90° T-L-T bond according to the Goodenough-Kanamori-Anderson (GKA) rules.⁶ Deviations from the GKA rules are known for CuGeO_3 due to the presence of side groups.⁷

Recently, the compound MgVO_3 was proposed as a candidate for a model spin-chain system and magnetic susceptibility measurements were presented.⁴ The data suggest short range antiferromagnetic spin correlations with the constant of the high-temperature Curie-Weiss law $\theta \approx -100$ K. The data were analyzed within a one-dimensional (1D) spin- $\frac{1}{2}$ Heisenberg model with the nearest neighbor J_1 and the next-nearest neighbor J_2 exchange couplings, and a frustration $\alpha = J_2/J_1$ close to the critical value⁸ $\alpha_c = 0.24$ was found. Here we present band-structure calculations for this compound and a corresponding orbital and tight-binding (TB) analysis.

The base-centered orthorhombic crystal structure of MgVO_3 was determined by Bouloux *et al.*⁹ and is shown in Fig. 1. It consists of edge-sharing VO_2 chains running along the *y* direction which are coupled in the *x* direction by V-O-O-V bonds. For a convenient presentation of the orbital analysis the coordinate system is rotated 90° about the *x* axis against the standard one¹⁰ so that the space group reads as $Bm2_1b$ instead of $Cmc2_1$ given in Ref. 9.

One notes a slight tilting of the VO_5 pyramids out of the *z* direction and an asymmetric coordination of V and two pairs of the nearest O1 ions. If one distorts the structure in a

way depicted in Table I both the tilting and the asymmetry are removed, a center of inversion appears, and the space group becomes $Bmmb$. The distortion preserves the Bravais lattice as well as the number and the crystallographic equivalence of the atoms in the primitive unit cell. In particular it means that the lower symmetry of the real structure produces no dimerization which would result in some additional gaps in the electronic spectrum. All the following results were obtained using the distorted model structure, because this simplification considerably reduces the computational efforts, and, as we have checked for the non-spin-polarized

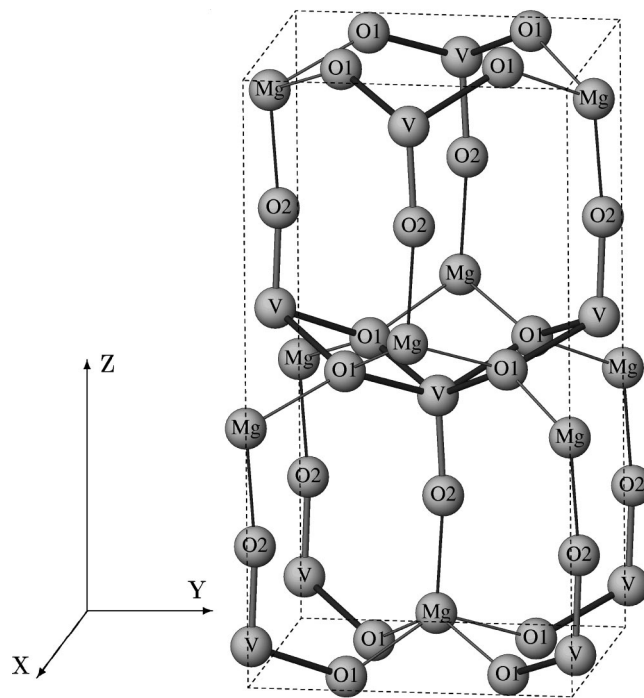


FIG. 1. Crystal structure of MgVO_3 . The dashed lines depict the Bravais unit cell. The lattice parameters of the cell are $a = 5.243$ Å, $b = 5.293$ Å, and $c = 10.028$ Å.

TABLE I. The Wyckoff positions of atoms in MgVO_3 .

Atom	Real structure			Model structure		
	x	y	z	x	y	z
Mg	0	0	0.4267	0	0	0.4267
V	0	0.011	0.0686	0	0	0.0686
O1	0.2383	0.264	-0.005	0.2383	0.25	0
O2	0	0.025	0.2330	0	0	0.2330

case, the deviation from the results obtained with the real crystal structure is negligible.

The calculation of the band structure was performed using the full-potential nonorthogonal local-orbital minimum-basis bandstructure scheme (FPLO) within the local spin-density approximation (LSDA).¹¹ The calculation was nonrelativistic, and the exchange and correlation potential was taken from Ref. 12. The set of valence orbitals was chosen to be Mg: $3s3p3d$, V: $3s3p4s4p3d$ and O: $2s2p3d$. The inclusion of the vanadium $3s3p$ states turned out to be unavoidable since the V-O2 distance of about $3.11a_0$ is small enough to yield a slight overlap of these states. The oxygen and magnesium $3d$ orbitals were taken to increase the basis completeness; though being not occupied they contribute to the overlap density. The extent of the basis orbitals, controlled by a confining potential $(r/r_0)^4$, was optimized with respect to the total energy.

In our calculation the Bloch state $|\mathbf{k}\nu\rangle$ is composed of overlapping atomiclike orbitals $|Lij\rangle$ centered at the atomic sites j in the unit cell i with coordinates \mathbf{R}_{ij} :

$$|\mathbf{k}\nu\rangle = \sum_{Lij} C_{Lij}^{\mathbf{k}\nu} e^{i\mathbf{k}\mathbf{R}_{ij}} |Lij\rangle, \quad (1)$$

with the normalization condition $\langle \mathbf{k}\nu | \mathbf{k}\nu \rangle = 1$. L stands for $\{nlm\sigma\}$ denoting the main, orbital, magnetic quantum numbers, and the projection of spin, respectively.

We have performed three kinds of computation: one non-spin-polarized and two spin-polarized with collinear and antiferromagnetic spin polarization at the neighboring in-chain vanadium ions. In the last case we assumed ferromagnetic order along the x and z directions. In both spin-polarized calculations we have found magnetic (ferro- and antiferromagnetic) solutions with the total energy being about 0.22 eV per formula unit lower than that of the paramagnetic solution of the non-spin-polarized calculation. The LSDA accuracy does not allow us to determine which of the magnetic states is preferable. The magnetic moment $\langle n_{\uparrow} - n_{\downarrow} \rangle \mu_B$ of the vanadium ion in both magnetic solutions is close to the saturated value $1\mu_B$. The magnetic moments of the other ions are much smaller, the only appreciable one occurs at apex oxygen (O2) having a value of about $0.05\mu_B$ and being directed opposite to the moment of the neighboring vanadium ion.

The results of all three calculations are presented in Fig. 2. The paramagnetic solution has metallic character with a half-filled conduction band at the Fermi level, whereas the band splits in two in the magnetic solutions and an insulator gap opens, being about 0.5 eV and 0.8 eV in ferro- and antiferromagnetic cases, respectively. However, it can be expected that the real gap is caused mainly by the electron

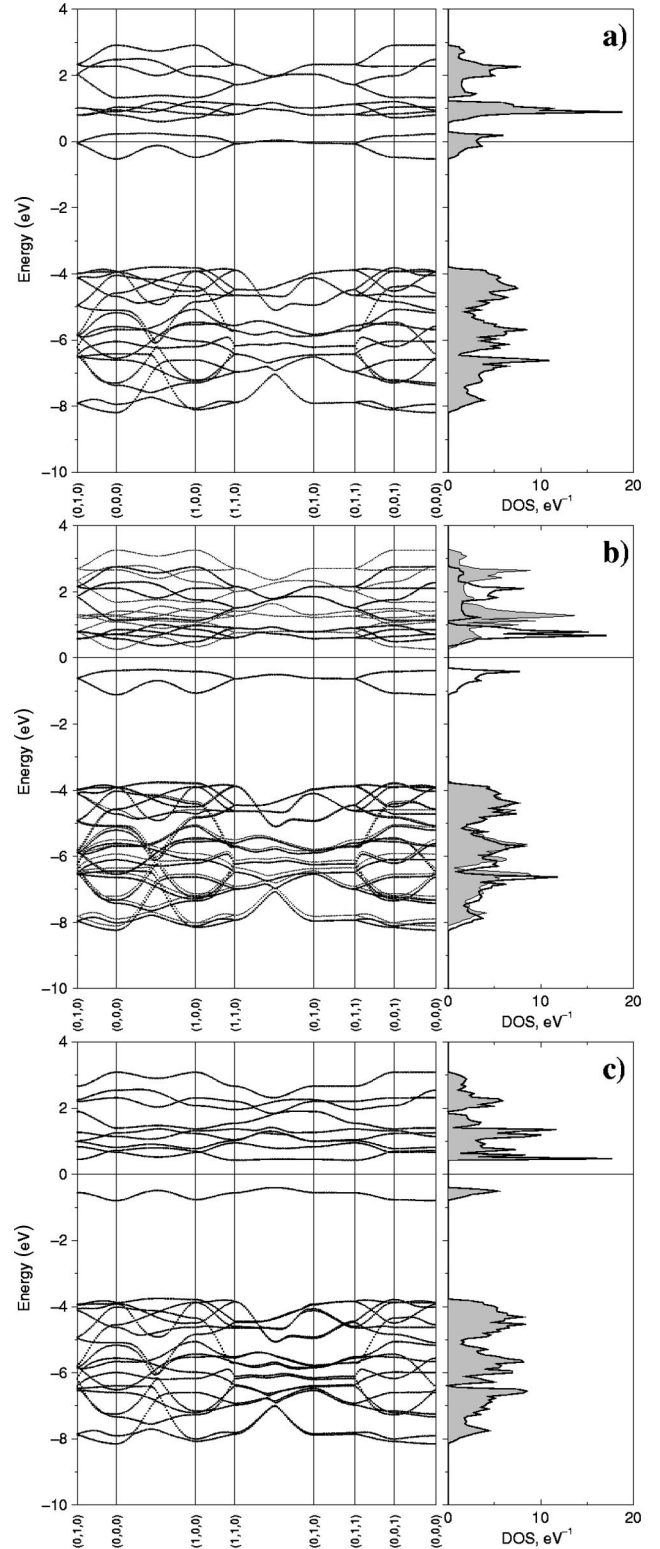


FIG. 2. Band structure and density of states of MgVO_3 for the paramagnetic (a), ferromagnetic (b), and antiferromagnetic (c) solutions. The symmetry point coordinates of the B -base centered orthorhombic Brillouin zone are given in units $\pi(2/a, 1/b, 2/c)$. The majority- and minority- (tinier dots and shaded DOS) spin parts are shown.

correlation and is considerably larger than the one produced by the magnetic ordering. The correlation gap should persist in the paramagnetic case as well.

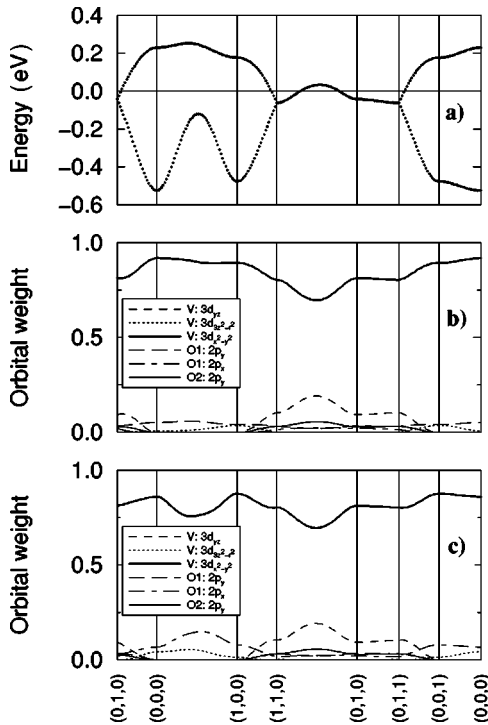


FIG. 3. Dispersion (a) and orbital weights of the upper (b) and lower (c) parts of the band crossing the Fermi level in the paramagnetic solution. The coordinates of k points are given in the same units as in Fig. 2.

For a deeper understanding of the electronic structure we have performed an orbital analysis for the paramagnetic case. The weight $W_{Lj}^{k\nu}$ of the orbital $|Lj\rangle$ in the Bloch state $|\mathbf{k}\nu\rangle$ (Eq. 1) was taken as

$$W_{Lj}^{k\nu} = \sum_i |C_{Lij}^{k\nu}|^2. \quad (2)$$

The sum of all weights $\sum_{Lj} W_{Lj}^{k\nu}$ is approximately unity, with some deviation due to the nonorthogonality of the basis orbitals. Actually the orbital weights were normalized with respect to the sum.

According to the analysis, the valence bands consist of a lower oxygen $2p$ -orbital complex which is separated by 3 eV from upper vanadium $3d$ orbitals (Fig. 2). The $3d$ orbitals are split according to the standard crystal-field rules. At $(0,1,0)$ their energy rises in the order: $d_{x^2-y^2}$, d_{yz} , d_{zx} , $d_{3z^2-r^2}$, d_{xy} . Only the lowest $3d_{x^2-y^2}$ orbital is partially occupied, being half filled with two electrons per two vanadium atoms in the primitive unit cell. The corresponding band (Fig. 3) is very narrow having a width of only 0.8 eV. The weight of the V: $3d_{x^2-y^2}$ orbital in the band is larger than 70%, but there are considerable contributions up to 20% from the O1: $2p_x$ and the V: $3d_{yz}$ orbitals, as well as smaller contributions from some other orbitals.

Comparing the situation with that in cuprates having the edge-sharing CuO_2 chains (Li_2CuO_2 or CuGeO_3) one observes an important distinction: in the cuprates the relevant Cu: $3d$ orbital is directed towards the oxygen ions, whereas in the present case it is directed towards the neighboring vanadium ions. It implies an indirect superexchange mechanism via the intermediate ligand in the cuprates but probably

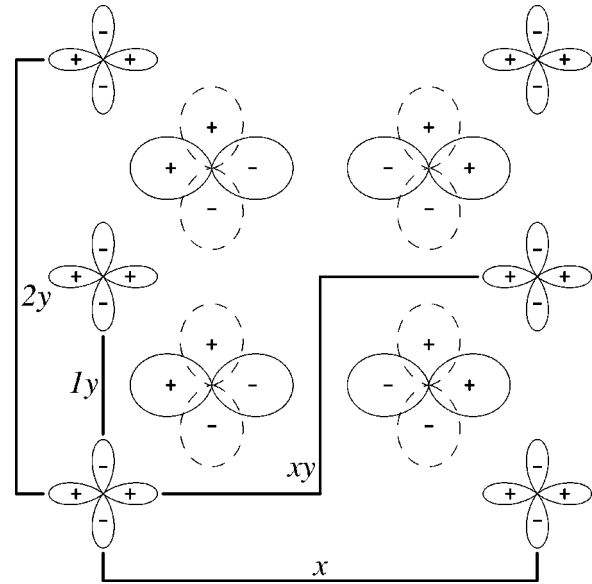


FIG. 4. Relevant V: $3d_{x^2-y^2}$ and O1: $2p_{x,y}$ orbitals coupling the spins in chain y direction and in the orthogonal x direction and the chosen in-plane transfer paths. The orbital phases correspond to the Γ point.

a dominant direct exchange process between neighboring vanadium ions and a much smaller superexchange hopping to the second in-chain neighbor in MgVO_3 . Let us note that the different coordination of the relevant $3d$ orbital in vanadates and cuprates with similar crystal structure has to be a rather common feature, because in vanadates the energetically lowest $3d$ orbital is half filled in contrast to the highest one in cuprates.

The coupling between the neighboring chains occurs mainly in the xy plane via the intermediate O1: $2p_x$ orbitals. This is manifested by the strong dispersion along the $(k_x, 0, 0)$ direction (Fig. 3) of the lower part of the band, which has a remarkable contribution from the orbital, whereas the upper part having a contribution only from the O1: $2p_y$ orbital is almost dispersionless. Figure 4 showing the relevant orbitals at the Γ point illustrates the interchain coupling via σ bonds of neighboring O1: $2p_x$ orbitals.

To quantify the result a TB analysis has been performed for the relevant band of the paramagnetic solution. The hopping processes to the nearest (t_{1y}) and the next nearest (t_{2y}) in-chain neighbors, as well as two hopping processes (t_x, t_{xy}) to the next chain and one (t_{xyz}) possible coupling in the z direction were taken into account:

$$E_0 - E_{\mathbf{k}} = 2t_{1y} \cos k_y \frac{b}{2} + 2t_{2y} \cos k_y b \\ + 2t_x \cos k_x a + 4t_{xy} \cos k_x a \cos k_y \frac{b}{2} \\ + 8t_{xyz} \cos k_x \frac{a}{2} \cos k_y \frac{b}{2} \cos k_z \frac{c}{2},$$

yielding the following parameters (in meV): $t_{1y} = 125$, $t_{2y} = 20 \dots 26$, $t_x = 50$, $t_{xy} = 20$, and a tiny value of 3 for t_{xyz} . The data confirm that the ratio t_{2y}/t_{1y} , a measure for the frustration in the chain direction, is much smaller than the

corresponding value for CuGeO_3 and Li_2CuO_2 .^{13,14} It should be noted that the parameter t_{1y} is much larger than the corresponding interladder hopping in NaV_2O_5 given in Ref. 15, probably due to a mutual compensation of different transfer paths in the ladder compound.

An estimate of the corresponding exchange integrals of the effective Heisenberg Hamiltonian

$$\hat{H} = \frac{1}{2} \sum_{ij} J_j \mathbf{S}_i \mathbf{S}_{i+j}$$

can be performed in the one-band Hubbard description, which gives an antiferromagnetic exchange of roughly $J_j = 4t_j^2/U$ with a value of U still to be determined. Using the experimental value of $J_{1y} \approx 10$ meV given in Ref. 4 one gets $U = 6.25$ eV which seems to be slightly overestimated. Most probably, additional ferromagnetic processes (possibly via the $3d_{yz}$ orbital or indirect processes via oxygen) have to be included to improve the estimate. Our TB analysis suggests a rather large value for J_x . It gives two-dimensional antiferromagnetic order with the frustration terms J_{2y} and J_{xy} (Fig. 4). Though t_{2y} and t_{xy} are of nearly the same value, due to the larger coordination number, J_{xy} dominates. In a simple mean-field approach one can define an effective frustration exchange $J_{\text{eff}} = 2J_{xy} + J_{2y}$ yielding an effective frustration J_{eff}/J_{1y} of roughly 0.1 which is a very preliminary analysis, however. The discrepancy with the value of 0.24 given in

Ref. 4 may result from an overestimate of J_{1y} in the one-band Hubbard model or from an inadequacy of the one-dimensional analysis of the experimental results performed in Ref. 4.

Thus, we have found that the VO_2 chains of MgVO_3 have indeed a spin- $\frac{1}{2}$ structure with the relevant $3d$ orbitals of the neighboring in-chain vanadium ions directed towards each other. It suggests a direct antiferromagnetic exchange process between the neighboring in-chain spins. A similar process was proposed for the interladder exchange coupling in MgV_2O_5 .¹⁶ The importance of the direct vanadium $d-d$ transfer was also anticipated in Ref. 17 for CaV_4O_9 , a compound with V-V distance slightly larger (3.00 \AA) than in MgVO_3 (2.96 \AA), where a value of 80 meV for the transfer was reported. Besides the direct exchange we have found some additional superexchange terms which give rise to the coupling between the chains in the x direction and to the frustration. The dominant frustration occurs between the neighboring chains in contrast to the naive picture of the frustration due to the next-nearest in-chain neighbor superexchange. It suggests that the experimental data require an analysis in the framework of a two- rather than a one-dimensional Heisenberg model.

We thank Christoph Geibel for useful discussions. I.C. and R.H. acknowledge the financial support of the Max Planck Society and the INTAS-RFBR (Grant No. 97-11066).

¹E. Dagotto and T.M. Rice, *Science* **271**, 618 (1996).

²K.M. Kojima *et al.*, *Phys. Rev. Lett.* **78**, 1787 (1997).

³Y. Mizuno *et al.*, *Phys. Rev. B* **57**, 5326 (1998).

⁴E. Morr e, C. Geibel, and U. L ow (unpublished).

⁵H. Rosner *et al.*, *Phys. Rev. B* **56**, 3402 (1997).

⁶P.W. Anderson, *Solid State Phys.* **14**, 99 (1963).

⁷W. Geertsma and D. Khomskii, *Phys. Rev. B* **54**, 3011 (1996).

⁸K. Okamoto and T. Nomura, *Phys. Lett. A* **169**, 433 (1992).

⁹J.-C. Bouloux, I. Milosevic, and J. Galy, *J. Solid State Chem.* **16**, 393 (1976).

¹⁰*International Tables for Crystallography* (Kluwer Academic Publishers, Dordrecht 1995).

¹¹K. Koepernik and H. Eschrig, *Phys. Rev. B* **59**, 1743 (1999).

¹²J.P. Perdew and A. Zunger, *Phys. Rev. B* **23**, 5048 (1981).

¹³R. Weht and W.E. Pickett, *Phys. Rev. Lett.* **81**, 2502 (1998).

¹⁴H. Rosner, R. Hayn, and S.-L. Drechsler, *Physica B* **259-261**, 1001 (1999).

¹⁵H. Smolinski *et al.*, *Phys. Rev. B* **57**, 5326 (1998).

¹⁶P. Millet *et al.*, *Phys. Rev. B* **57**, 5005 (1998).

¹⁷W.E. Pickett, *Phys. Rev. Lett.* **79**, 1746 (1997).